

ACOUSTO-OPTIC MODULATION OF LIGHT

https://doi.org/10.1070/QEL17361

Broadband fibre-pigtailed acousto-optic frequency shifter

M.M. Mazur, L.I. Mazur, A.V. Ryabinin, V.N. Shorin

Abstract. **A two-crystal fibre-pigtailed acousto-optic frequency shifter has been developed and investigated. An optimal configuration of acousto-optic cells is chosen. A two-crystal acousto-optic frequency shifter of 785-nm laser radiation in the range from 156 to 196 MHz, with single-mode polarisation maintaining fibres at the input and output, is described. Some recommendations are given how to improve the shifter transmission coefficient and increase the frequency shift range.**

Keywords: *laser frequency shift, acousto-optic interaction, fibre beam input, anisotropic diffraction.*

1. Introduction

Acousto-optic frequency shifters (AOFS's) are widely used in fountain frequency standards. In addition, AOFS's (highly diverse in frequency range and diffraction) are applied to design light frequency stabilisation systems, light frequency references, and light frequency measurement systems [1–4].

Currently, fibre-pigtailed acousto-optic modulators (AOMs) are produced by a number of companies: Brimrose Corporation of America (United States), Gooch & Housego PLC (United Kingdom), IPG Photonics (Russia), etc. However, these AOMs, being used as AOFS's, have a frequency shift tuning range of 2–5 MHz. Modern AOFS's can operate in a wide frequency range, which is provided by mechanical adjustment or using a scheme with several additional optical elements, including cat's eye (objective), quarter-wave phase plate, and polarisation separator [5].

In this paper, we report the results of studying a new-type AOFS: a two-crystal acousto-optic frequency shifter (TCAOFS), which extends significantly the range of laser frequency shift with a fibre-pigtailed output and input.

2. Choice of frequency shifter configuration

The frequency range of fibre-pigtailed AOFS is determined by the minimum among three frequency ranges [6]: the frequency range of ultrasonic cell matching with the RF channel, Δf_{match}; the frequency range of acousto-optic interaction synchronism, Δf_{syn}; and the frequency range beyond which the transmission coefficient decreases due to the light spot displacement from the fibre end face, Δf_{shift}. With a lithium niobate crystal used as an ultrasonic converter and optimal choice of an adhesive layer between the converter and acousto-optic cell (AOC), the Δf_{match} value may amount to one and a half octaves of the converter centre frequency [7]. The frequency range of acousto-optic interaction synchronism, Δf_{syn}, depends strongly on the configuration of this interaction and exceeds an octave for a deflector with anisotropic diffraction [8]. The limitation of the range Δf_{shift} for AOFS's with a fibre-pigtailed output is as follows: a change in frequency makes the light beam at the AOC output deviate from its initial direction by an angle dependent of the ultrasonic frequency. The beam waist displacement at the collimator output with respect to the fibre cable core is proportional to the variation in frequency. At a level of –4 dB [6] we have

$$\Delta f_{\text{shift}} = \frac{DV}{F\lambda}, \tag{1}$$

where D is the fibre core diameter, V is the ultrasonic wave velocity, F is the collimator focal length, and λ is the light wavelength.

In the case of a TCAOFS, the light beam at the second-AOC output retains its initial propagation direction with a high accuracy in the entire frequency tuning range [9]. However, the beam is displaced when the ultrasonic frequency is adjusted due to the angular deviation in the gap between two AOCs. Since the parallel beam shift is proportional to the change in frequency, the frequency range Δf_{shift} becomes limited. Obviously, the Δf_{shift} value can be increased by locating AOCs maximally close to each other (thus reducing the light beam displacement) and choosing an output collimator minimally sensitive to the parallel beam displacement relative to the collimator axis.

For an AOFS with fibre-pigtailed inputs, an important factor is the preservation of the angular and spatial positions of the output beam when tuning ultrasonic frequency rather than the directions of the entering and emerging beams. A wide range of variation in the laser frequency shift without changing the beam propagation direction can be ensured by applying successive beam diffraction from two identical AOCs [10].

Note that this AOFS configuration maintains the output beam propagation direction when the ultrasonic frequency changes.

It is convenient to use an anisotropic deflector to implement a TCAOFS AOC. The configuration of a nonaxial anisotropic deflector in a uniaxial crystal can be provided in two ways [8]. In one of these versions the wave vector of the

M.M. Mazur, L.I. Mazur, A.V. Ryabinin, V.N. Shorin All-Russian Scientific Research Institute of Physical-Technical and Radiotechnical Measurements (VNIIFTRI), 141570 Mendeleevo, Moscow region, Russia; e-mail: ryabinin.nn@yandex.ru

Received 13 May 2020
Kvantovaya Elektronika **50** (10) 954–956 (2020)
Translated by Yu.P. Sin'kov

input optical beam makes a smaller angle with the optical axis than the wave vector of the output ordinary wave. The situation with the other version is vice versa. For the configuration of an anisotropic deflector based on an optically positive crystal, for example, TeO_2, the input beam must be extraordinary. Figure 1 shows the vector diagram of these versions of acousto-optic interaction for ultrasonic waves propagating in the same direction.

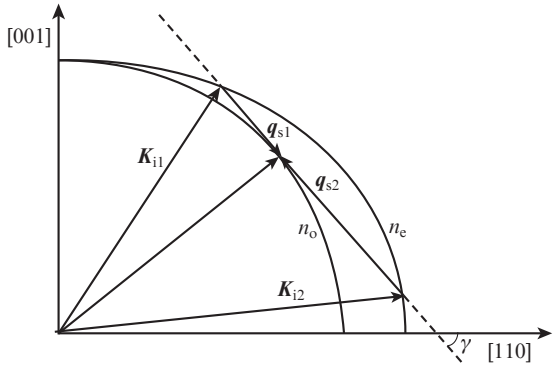

Figure 1. Vector diagram of acousto-optic interaction for two configurations of acousto-optic deflector: $\boldsymbol{K}_{i1}$ and $\boldsymbol{K}_{i2}$ are the wave vectors of incident extraordinary light wave; $\boldsymbol{K}_d$ is the wave vector of diffracted ordinary light wave; $\boldsymbol{q}_{s1}$ and $\boldsymbol{q}_{s2}$ are the wave vectors of sound waves; γ is the angle characterizing the sound wave propagation direction; [001] and [110] are the crystallophysical directions; and n_o and n_e are, respectively, the refractive indices of TeO_2 crystal for ordinary and extraordinary light waves.

Both interaction versions can be applied to a TCAOFS based on a paratellurite crystal. However, if the laser frequency shift must be small, the angle γ should also be small, and the light waves propagating in the cell make a small angle with the [001] axis. Hence, one must take into account the ellipticity of these waves because of the crystal gyrotropy. It was shown in [11] that for a TCAOFS based on a TeO_2 AOC with an interaction diagram corresponding to an extraordinary input wave with a wave vector $\boldsymbol{K}_{i2}$ (Fig. 1), the spatial shift of a doubly diffracted beam, measured on a base of 3400 mm at a laser frequency shift from 170 to 256 MHz, was less than 0.5 mm. Hence, the light beam angular displacement in a TCAOFS is below 0.5′, and one can conclude that this TCAOFS can also be used to design a wide-range fibre frequency shifter.

A TCAOFS breadboard with fibre collimators at the input and output was fabricated based on a TeO_2 AOC with the interaction geometry corresponding to the incident extraordinary wave with a wave vector $\boldsymbol{K}_{i1}$. The cells were calculated and made antireflective for 785-nm radiation.

The optical scheme of a wide-range laser TCAOFS with fibre inputs is presented in Fig. 2. Ultrasonic converters (*3*) were 3 mm long and 2 mm high. To simplify the fabrication technology, the ultrasonic converters/shifters, made of a $LiNbO_3$ crystal (the Y+163° cut) were attached to acousto-optic waveguides via cyanoacrylate glue without any additional acoustic-matching layer, which limited the ultrasound excitation frequency band Δf_{match}. The dotted lines indicate the ultrasonic-wave propagation region. The ultrasonic propagation direction is determined by the wave vector $\boldsymbol{q}_{s1}$, and the angle γ in the fabricated AOCs is 9.5°.

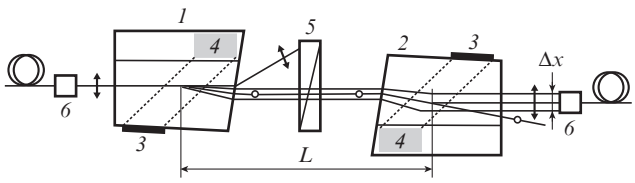

Figure 2. Optical scheme of TCAOFS: (*1*, *2*) AOCs; (*3*) ultrasonic converters; (*4*) ultrasonic wave absorbers; (*5*) polariser; (*6*) input and output collimators; the signs ○ and ↕ denote the light polarisation state.

The light beam displacement Δx in the gap between two AOCs, with the refractive indices of the AOC and polarisation divider disregarded, can be described by the expression

$$\Delta x \approx \frac{L\lambda\Delta f}{V_{s1}}, \tag{2}$$

where L is the distance between the regions of AO interaction in the AOC, V_{s1} is the velocity of a shear wave with a wave vector $\boldsymbol{q}_{s1}$, and Δf is the RF signal tuning range. For the TCAOFS under study, $L \approx 2$ cm and $V_{s1} = 6.64 \times 10^4$ cm s^{-1}; thus, at $\lambda = 0.785$ μm and $\Delta f = 20$ MHz, $\Delta x \approx 0.5$ mm.

When using the version with introduction of an extraordinary wave corresponding to the wave vector $\boldsymbol{K}_{i1}$, the centre phase-matching frequency is about 90 MHz. The AOC optical faces were inclined so as to make the radiation diffracted in the first AOC propagate parallel to the incident beam at this frequency.

3. Measurement results and analysis

A fibre laser LP785-SAV50, generating unpolarised light, was used as an emitter. To make the radiation polarised, a polarisation beam splitter was installed on a U-shaped assembly platform FBP-B-FC, equipped with fibre ports. The radiation was supplied (through a single-mode polarisation-maintaining fibre) to the TCAOFS input connector and transformed (by a PAF2-7B collimator, *6*) into a quasi-parallel beam, which was successively diffracted in two AOCs (*1* and *2*) and then introduced (through output collimator *6*) into a single-mode polarisation-maintaining fibre.

The results of measuring the diffraction efficiency η in each AOC and the transmission coefficient T of doubly diffracted radiation, with allowance for the loss in the polarisation beam splitter, are shown in Fig. 3. With AOC installed in the TCAOFS housing, the maximum diffraction efficiency in the cells (curves *1*, *2*) did not exceed 80%–84%, which is apparently related to the error in aligning the ultrasonic and light beams in height, because, in the case of AOC location beyond the housing, the diffraction efficiency reached 96% at an RF signal power of about 100 mW. Curve *3* corresponds to the transmission coefficient for light passing through the input collimator, two AOCs, and polariser. Curve *4* corresponds to the light power transmission coefficient with allowance for the losses in the input collimator, two AOCs, and polarisation beam splitter and the loss at the radiation inlet into the fibre using an output collimator. For the TCAOFS with the chosen symmetric AOC arrangement, the tuning range of 20-MHz RF signal corresponds to a laser frequency shift by 40 MHz. It follows from these results that, for the TCAOFS under consideration, at the midpoint of the afore-

mentioned range, the losses in the two cells and polariser are about 2 dB; additionally, about 2 dB are lost when extracting radiation through the output collimator. Moreover, losses increase even more (by 2 dB) at the range boundaries with a change in the RF signal frequency by ±10 MHz relative to the range midpoint, which corresponds to a frequency shift by ±20 MHz.

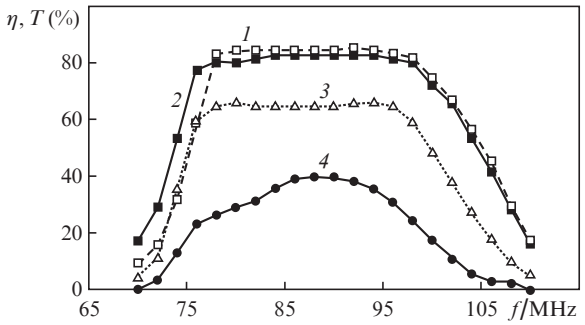

Figure 3. Dependences of the transmission characteristics of a TCAOFS and its combined parts on the RF signal frequency *f*.

A reasonable question arises: is there any possibility of increasing the TCAOFS transmission coefficient? As was mentioned above, improving the alignment of light and sound beams, one can reduce losses during acousto-optic diffraction, apparently, to a value no more than 1 dB during transmission through two AOCs. At the same time, the choice of appropriate collimators and their correct alignment should also reduce losses to a level below 1 dB when transmitting light through a collimator to a fibre at the midpoint of the aforementioned range. Additional studies must be performed to find out how the losses will change at the range boundaries and determine the maximum increase in the tuning range that can be achieved in this case.

4. Conclusions

A new type of a fibre-pigtailed acousto-optic frequency shifter – TCAOFS based on successive anisotropic diffraction in two AOCs – was developed and fabricated. The correctness of calculation prerequisites was demonstrated, and the TCAOFS operating capacity was confirmed.

A band of laser frequency shift of 40 MHz was achieved without mechanical adjustment and using additional optical elements (phase plate and cat's eye) with a fibre-pigtailed radiation input and output.

Acknowledgements. We are grateful to S.I. Donchenko, the General Director of the Federal State Unitary Enterprise VNIIFTRI, and A.V. Aprelev, the Head of the Research Department of Acousto-Optical Measurements and Laser Optoelectronics (NIO-9), for putting the research aimed at developing a broadband fibre-pigtailed AOFS.

References

1. Berdasov O.I., Khabarova K.Yu., Strelkin S.A., Belotelov G.S., Kostin A.S., Gribov A.Yu., Pal'chikov V.G., Kolachevskii N.N., Slyusarev S.N. *Al'm. Sovrem. Metrol.*, (1), 13 (2014).
2. Berdasov O.I., Gribov A.Yu., Strelkin S.A., Slyusarev S.N. *Al'm. Sovrem. Metrol.*, (11), 81 (2017).
3. Baryshev V., Epikhin V., Blinov I., Donchenko I. *Proc. 2016 IEEE Int. Frequency Control Symp.* (New Orlean, LA, USA, 2016) pp 205–208.
4. Baryshev V.N., Epikhin V.N. *Quantum Electron.*, **40** (5), 431 (2010) [*Kvantovaya Elektron.*, **40** (5), 431 (2010)].
5. Donley E.A., Heavner T.P., Levi F., Tataw M.O., Jefferts S.R. *Rev. Sci. Instrum.*, **76**, 063112 (2005).
6. Epikhin V.M. *Doklad na seminare NIOO9 FGUP VNII FTRI* (Report at the Seminar of the Research Department of Acousto-Optical Measurements and Laser Optoelectronics (NIO-9), Federal State Unitary Enterprise VNIIFTRI) (Mendeleevo, 2020).
7. Dieulesaint E., Royer D. *Elastic Waves in Solids. Applications to Signal Processing* (New York: Wiley, 1980; Moscow: Nauka, 1982).
8. Balakshy V.I., Parygin V.N., Chirkov L.E. *Fizicheskie osnovy akustooptiki* (Physical Principles of Acousto-Optics) (Moscow: Radio i Svyaz', 1985).
9. Mazur M.M., Mazur L.I., Shorin V.N. RF Patent No. RU 2648567 (priority date 24 May, 2017).
10. Mazur M.M. *Doctoral Diss.* (Moscow, Scientific and Technological Centre of Unique Instrument Engineering of the Russian Academy of Sciences, 2007).
11. Aprelev A.V., Mazur M.M., Mazur L.I., Shorin V.N. *Sb. dokl. IX mezhdunar. simp. 'Metrologiya vremeni i prostranstva'* (Proc. IX Int. Symp. "Metrology of Time and Space") (Mendeleevo, 2018) p. 201.